PHILOSOPHICAL TRANSACTIONS A

royalsocietypublishing.org/journal/rsta

Review

Cite this article: Chen X, Yan J, Deng L, Wu F, Wu L, Xu Y, Zhou L. 2021 Discovering the sky at the longest wavelengths with a lunar orbit array. *Phil. Trans. R. Soc. A* **379**: 20190566. http://dx.doi.org/10.1098/rsta.2019.0566

Accepted: 30 July 2020

One contribution of 16 to a discussion meeting issue 'Astronomy from the Moon: the next decades'.

Subject Areas:
cosmology, observational astronomy, space exploration, interstellar medium

Keywords:
lunar astronomy, radio astronomy, dark ages

Author for correspondence:
Xuelei Chen
e-mail: xuelei@cosmology.bao.ac.cn

Discovering the sky at the longest wavelengths with a lunar orbit array

Xuelei Chen[1], Jingye Yan[2], Li Deng[2], Fengquan Wu[1], Lin Wu[2], Yidong Xu[1] and Li Zhou[2]

[1]National Astronomical Observatories, Chinese Academy of Sciences, 20A Datun Road, Beijing 100101, People's Republic of China
[2]National Space Science Center, Chinese Academy of Sciences, Beijing 100190, People's Republic of China

XC, 0000-0001-6475-8863

Due to ionosphere absorption and the interference of natural and artificial radio emissions, astronomical observation from the ground becomes very difficult at the wavelengths of decametre or longer, which we shall refer to as the ultralong wavelengths. This unexplored part of the electromagnetic spectrum has the potential for great discoveries, notably in the study of cosmic dark ages and dawn, but also in heliophysics and space weather, planets and exoplanets, cosmic ray and neutrinos, pulsar and interstellar medium (ISM), extragalactic radio sources, and so on. The difficulty of the ionosphere can be overcome by space observation, and the Moon can shield the radio frequency interferences (RFIs) from the Earth. A lunar orbit array can be a practical first step to opening up the ultralong wave band. Compared with a lunar surface observatory on the far side, the lunar orbit array is simpler and more economical, as it does not need to make the risky and expensive landing, can be easily powered with solar energy, and the data can be transmitted back to the Earth when it is on the near-side part of the orbit. Here, I describe the discovering sky at the longest wavelength (DSL) project, which will consist of a mother satellite and 6–9 daughter satellites, flying on the same circular orbit around the Moon, and forming a linear interferometer array. The data are collected by the mother satellite which computes the interferometric cross-correlations (visibilities) and transmits the data back to the Earth.

THE ROYAL SOCIETY PUBLISHING

The whole array can be deployed on the lunar orbit with a single rocket launch. The project is under intensive study in China.

This article is part of a discussion meeting issue 'Astronomy from the Moon: the next decades'.

1. Introduction

Modern astronomical observations are conducted over a very wide range of wavelengths, from radio, through infrared, optical, ultraviolet, X-ray, to gamma-ray, and further supplemented by non-electromagnetic observations such as neutrinos and gravitational wave events. Each new observational domain brought many unexpected discoveries and greatly changed our view of the Universe. However, at the long wavelength end (frequency below 30 MHz), the sky has barely been explored (see e.g. [1–3] for a summary of the early observational efforts), as the ionosphere severely distorts and absorbs the electromagnetic wave, and radio frequency interferences (RFI) are also very strong and nearly omnipresent, thanks to the reflection of the ionosphere.

A number of early space missions, such as the IMP-6 [4], Radio Astronomy Explore (RAE)-1 [5] and RAE-2 [6,7] made low-frequency radio observations from space. Some solar system probes such as WIND and Cassini also carried low-frequency radio payloads. The data collected by these satellites showed that the Earth has strong natural radio emissions at the kilometric wavelengths (note this radiation is at a longer wavelength than that of dark ages observation), and as the artificial sources are much stronger than the radio astronomical sources, even with the ionospheric absorption, man-made radio frequency interferences are visible from space. However, the angular resolutions of these single receiver satellites are very poor. It is time to consider a new space mission to explore and reveal the mysteries of this wave band.

There are a number of options for a low-frequency radio space mission. Deploying satellites in orbit around the Earth is relatively simple and cheap to do, indeed the SunRise is such a mission [8], but the RFI from the Earth would be a major problem. An array on the Sun-Earth L2 point allows all-time monitoring of the whole sky, but it is also constantly exposed to the radio emission from the Earth, though reduced in magnitude by the distance. Launching the satellites and maintaining the array configuration around the unstable L2 point, determining their relative positions in widely separated sky directions, and transmitting the data back all require a substantial amount of resources both on board the satellite and on the ground, making the mission quite hard. Radio observation from the far side lunar surface is another option. A first experiment was carried out in 2018 by the Chang'e-4 (CE-4) lander [9]. For an array on the lunar surface, the imaging methods and tools developed for the ground-based radio astronomy could be readily used. However, a relay satellite is required to transmit the data back to the Earth, and furthermore, supplying energy for the lander during the half-month-long lunar night requires a special power source such as a radioisotope thermoelectric generator figure 1.

Making radio observations from the orbit around the Moon has a number of advantages, which makes it easier to realize in near term. The part of the orbit behind the Moon provides the perfect environment against the radio emissions from the Earth. The orbital period is about 2.3 h for an orbit of 300 km altitude, so the energy can be easily supplied with solar power. The data can be transmitted back to the Earth when the satellite is on the near side, without the need for another relay satellite, and the complicated landing and deployment are also avoided. Even a single lunar satellite could measure the global average spectrum (i.e. the spectrum of the radiation averaged over the whole sky). The DARE/DAPPER mission is such a concept [10,11] and may also detect strong radio sources by using the Moon as a moving screen. However, as the wavelength is very long, to achieve high angular resolution, it is natural to consider an interferometer array [12–14]. There was an attempt to try the lunar orbit array during the CE-4 mission. Two micro-satellites (Longjiang-1 and-2) piggy-backed on the rocket which launched the relay satellite for the CE-4 mission [15], but unfortunately, the Longjiang-1 satellite was lost shortly after the launch.

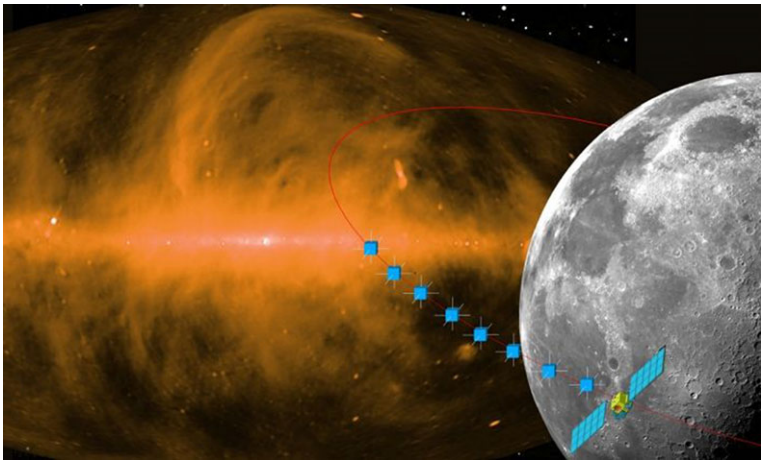

Figure 1. An artist's concept of the DSL mission. (Online version in colour.)

In this contribution, we describe the discovering the sky at longest wavelength (DSL) mission [16–18], which employs a linear array of satellites on an inclined circular orbit around the Moon to make interferometry observations and is currently under intensive study.

2. The science goals

As a first explorer mission, the main science objectives of the DSL are (i) to open up a new window of observation by mapping the sky and cataloguing the major sources at this wavelength, to reveal new astrophysical phenomena at this wavelength, and to discover the unknown unknowns; (ii) to explore the dark ages and cosmic dawn by making high-precision global spectrum measurements.

With the high-resolution map, we will see various objects shining in this unexplored wave band. They could be stars and planets, nebulae, quasar jets and relics, or galaxy cluster radio halos, to name just a few. The observation at this wavelength will provide new information about these objects. As a simple example of what can be learned from such observations, in figure 2, we show a simulated sky map at the 3 MHz, based on an extrapolation of maps at higher frequencies, with the emissivity given by an exponential disc model, and the expected absorption from the interstellar medium (ISM) using the NE2001 model [20]. The ISM is the matter that exists in the space between the star systems in the Galaxy, including gas in ionic, atomic and molecular form, as well as dust and cosmic rays. It provides the material from which the stars and planets form, and it is also constantly replenished with newly accreted gas as well as material and energy from stellar winds, planetary nebulae and supernovae. The ISM plays a crucial role in astrophysics; the very low-frequency observations of DSL will provide an excellent means of tracing the diffuse ionized ISM. A conspicuous feature of the figure is that the galactic plane, which is the brightest part of the sky at higher radio frequencies, becomes the darkest part of the sky (shown as blue-black colour), thanks to the strong absorption which becomes significant at this low frequency. This allows us to see the ionized gas around us. The local bubble, in which our solar system resides, is of particular interest, as it may have had some impact on the solar system for the last few million years. The dark spot in the map, which is created by a nearby HII region, may also provide a perfect place to study the production and propagation of the cosmic ray particles, as the radio emission of the cosmic ray electrons from behind the region is blocked.

The evolution of the Universe from the end of the hot Big Bang, through the dark ages, to the formation of the first luminous objects is only speculated. It remains a gap in our knowledge about cosmic history. Furthermore, the large comoving volume and perturbations still undergoing

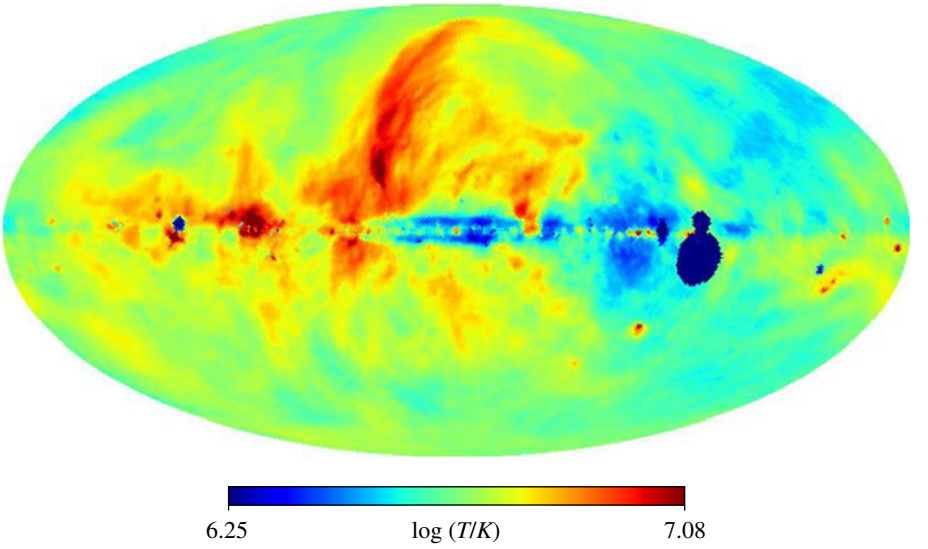

Figure 2. A simulated sky map at 3 MHz (from Y. Cong *et al.*, *in preparation* [19]). (Online version in colour.)

linear evolution during these epochs are also a precious trove of information for the high-precision study of the primordial fluctuations and cosmic origin. However, the strong foreground at low frequency means that extremely high sensitivity is required in order to measure these primordial fluctuations, which is far beyond the capability of the present experiment. A first step toward the study of the dark age and cosmic dawn can be made with the global spectrum measurement. The signal-to-noise ratio of a global spectrum detection is independent of the receiver collecting area, hence could be carried out with a single antenna. During cosmic dawn, the Lyman alpha photons produced by the first stars couple the spin temperature of the hydrogen gas to its kinetic temperature, and the latter is cooled by the expansion of the Universe and heated by X-ray radiation of first black holes. These processes may produce a deep absorption trough in the global signal (figure 3) [21,22], and features in the global spectrum have been searched by a number of ground-based experiments, such as the EDGES, SCI-HI and SARAS. Unexpectedly, an absorption as deep as twice that allowed by the standard theory was reported by the EDGES experiment [23]. It has been speculated that such features could be explained by some exotic processes, such as baryon-dark matter scattering [24], but it is crucial to verify the result with an independent experiment which is least affected by various systematic effects, e.g. ground plane reflection [25]. In a lunar orbit experiment, the problems of ionosphere distortion can be avoided, and although the Moon does reflect radio waves, the much larger height of the satellite means that it is unlikely to produce fake absorption features on the scales of interest. We note here that although the observation of lunar orbit has these advantages, the whole measurement is still highly challenging, because no antenna has a completely frequency-independent beam, and the spatial structure may be convoluted to the measured global spectrum to produce false absorption features. A sophisticated data analysis method needs to be developed to reduce such an effect and check the validity of the detected features [26]).

Maps made by the DSL at lower frequencies would be useful for further studies on the dark age, revealing for the first time the radiation sources at these frequency ranges, and helping with the design of future larger missions.

Finally, the mission may detect varying radiation from within the solar system, such as the Type II/III solar bursts, or the low-frequency radio burst of Jupiter and other planets, though the array is perhaps too small to detect the burst from other stars or exoplanets. For a linear array such as the DSL, the spatial structure of such a varying source could be obtained only in one

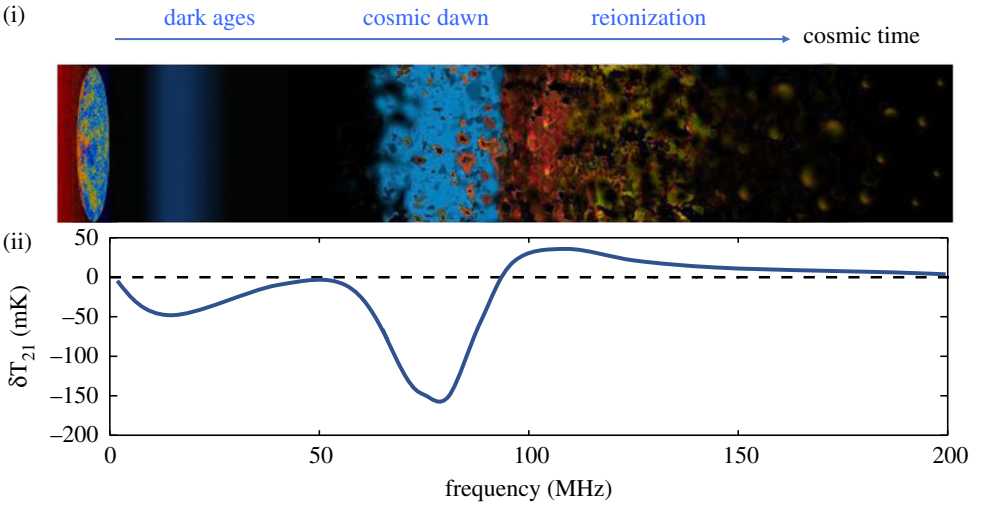

Figure 3. The 21 cm global spectrum (ii) and fluctuation signals (i) throughout the cosmic history. (Online version in colour.)

direction. Still, the angular resolution of the array may allow it to resolve heretofore unknown compact structure in the burst.

Throughout the history of radio astronomy, there have been numerous examples of unexpected discoveries, such as the detections of radio emission from celestial radio sources in continuum (e.g. pulsars, Fast Radio Bursts) and spectral lines (e.g. OH masers). Each radio astronomy instrument built with at least one unique capability—sensitivity, spectral, time or angular resolution and spectrum coverage—is practically guaranteed outstanding discoveries. There is every reason to expect that a prospective space-based ultra-long wavelength facility will continue the trend of delivering unexpected discoveries.

3. Basic concept of the lunar orbit array

The proposed array consists of a constellation of satellites circling the Moon on nearly identical orbits, forming a linear array while making interferometric observations. The linear configuration allows the array to stay in a relatively stable configuration in orbit, and relative positions of each satellite can be measured accurately with very limited instrumentation; a star sensor camera for angular measurement, and a microwave communication link for distance measurement, the latter of which is also used for inter-satellite data communication and synchronization. The present design of the array adopts a circular orbit of 300 km height which is shown by orbital simulation to be sufficiently stable against lunar gravity perturbations. A lower orbit has the advantage that it allows longer shielding time against the Earth, which is especially important below 0.5 MHz, as the AKR region extends several Earth radii [27], but due to the greater perturbation of the lunar gravity field the orbit management is harder.

The constellation will include a mother satellite and a number of (tentatively set as nine) daughter satellites. One of the daughter satellites will be dedicated to the global spectrum measurement at the higher frequency band of 30–120 MHz, with the aim of probing the 21 cm signal from the cosmic dawn. The other eight daughter satellites will perform the spectrum and interferometric imaging observation below 30 MHz. The mother satellite, flying in the front or end of the linear array, will collect the digital signals from each daughter satellite and perform the interferometric cross-correlations, store the results, and transmit the data back to Earth when it is in the near-side part of the orbit. The daughter satellites will be docked on the mother satellite during launch and lunar transfer, then sequentially released after entering the lunar orbit to form the linear array. The assembly of mother and daughter satellites is shown in figure 4.

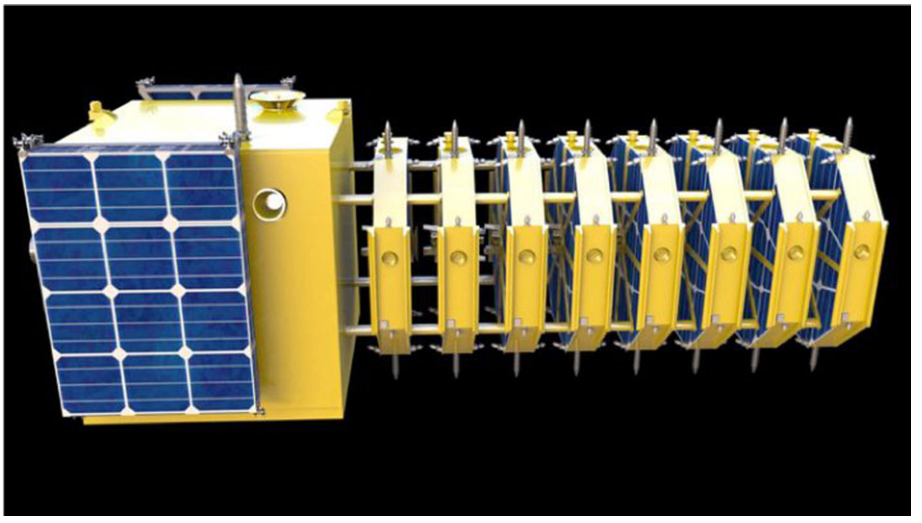

Figure 4. The mother and daughter satellites assembly. The total weight at launch is about 1400 kg, with 600 kg propellant. The dry weight of the mother satellite is about 330 kg, and each daughter satellite 50 kg. (Online version in colour.)

Each daughter satellite is equipped with its own propulsion system, so that it could make small positional adjustments in orbit.

The upper part of the mother satellite is equipped with deployable solar panels, a high gain antenna for ground communication, and other sensors and antennas. The lower part of the mother satellite carries the daughter satellites. After entering the lunar orbit and being released, the satellites will naturally have some velocity differences under the irregular gravity field of the Moon. However, the formation is automatically controlled to keep the linear array stable.

Each daughter satellite is a thin octagonal slab with a diameter of about 1 m, and the slab surface allows a relatively large area for solar cells. The regular smooth geometry is designed to simplify the modelling of the antenna response. One of these is dedicated to the high-precision measurement of the global spectrum in the high band (30–120 MHz) for cosmic dawn. A monopole cone antenna with a ground plate is selected for the measurement of this frequency band. The antenna is designed to have a nearly frequency-independent beam and to be thermally stable and mechanically rigid. A precise calibration system will be embedded into the receiver as a core module, and differential measurement will be used in the receiving system. In order to detect the trough of 21 cm absorption, the goal is to reach an error of 5 mK on the brightness temperature at 75 MHz within the mission duration; this would allow detection of the cosmic dawn signal at SNR greater than 10. Reaching this accuracy requires greater than 60 dB pass-band calibration. For foreground subtraction, the full band needs to be observed with a spectral resolution of 1 MHz.

Each of the other eight daughter satellites carries three orthogonal short dipole antennas, a receiver, a digitizer and a low-frequency interferometer and spectrometer (LFIS). The daughter satellites are stabilized with respect to the Moon, with a pointing accuracy of the three axes better than 1°, attitude stability better than 0.1°/s and attitude measurement better than 0.01°. Limited by the inter-satellite communication bandwidth, a selection of 30 narrow bands (each with 8 kHz bandwidth) within the 0.1–30 MHz range will be used for interferometry.

The inter-satellite communication between each daughter satellite and the mother satellite is provided by a Ka-band microwave link, which also serves to synchronize the clocks on each satellite. In addition, it also measures the distance from each daughter satellite to the mother satellite. The angular position of a daughter satellite with respect to the mother is measured by having the star sensor camera on the daughter to take photographic shots in the direction of the mother, which carries an LED light array for identification against the star background. This

system (called the inter-satellite dynamic baseline apparatus, ISDBA) is required to achieve a positioning precision of 1 m in each direction (1/10 wavelength at 30 MHz), which translates to a ranging precision of 1 m, with the corresponding clock synchronization precision of 3.3 ns, and an angular precision of 10 urad at 100 km.

As the constellation of satellites orbits the Moon, multiple baseline vectors are formed between the eight daughter satellites and generate concentric rings in the uv plane (u, v and w are Cartesian coordinates in units of wavelength, with w usually pointing toward the target direction). The gaps between the rings can be partially filled by varying the spacing between the satellites, or by bandwidth synthesis. It should be emphasized that the satellites do not need to have fixed relative positions, but as long as the positions can be determined accurately enough, the interferometry could work. The short dipole antennas are sensitive more or less in all directions, and the Moon only shields a small fraction of the sky; therefore, there is a mirror symmetry between the two sides of the orbital plane that cannot be broken using the data from a single orbit alone. However, the orbital plane processes for 360 degrees in 1.29 years, so after a few orbits, three-dimensional distribution of the baselines will be formed, and thus sources can in principle be determined by combining these measurements from different aperture planes. After a full-period precession, the baselines will fill a three-dimensional 'doughnut' shaped structure, and a sky image can be reconstructed by linear inversion from the three-dimensional visibility dataset [17].

The angular resolution of an interferometer array is determined by the longest baseline. However, at low frequencies, the resolution is also limited by the broadening effect induced by scattering in the ISM as well as in the interplanetary medium (IPM) [28]. The maximum baseline for DSL is set to be 100 km, corresponding to a resolution of 0.17 degree at 1 MHz, which is better than the limit set by the scattering. Except for the radio recombination lines and molecular lines detections, most of the known radiation mechanisms at low frequencies such as the synchrotron and free-free radiation produce smooth continuum radiation, for which high spectral resolution is not needed. Also, the foreground subtraction of the redshifted 21 cm line also only requires a moderate spectral resolution. However, fine spectral resolutions are still required in order to keep frequency coherence, because the baselines are moving as the satellite array circulating the Moon.

Detection sensitivity at long wavelengths is strongly influenced by the confusion limit, which limits the identification and measurement of individual sources, and occurs when there is more than one source in every 30 synthesized beams. Based on an extrapolation of the VLA 74 MHz and the Parkes 80/178 MHz source counts, we estimate that at 1 MHz, the confusion limit will be reached after observing with eight antennas for a few weeks, but at a higher frequency, the mapping sensitivity will be primarily limited by integration time, not by confusion.

4. Key technologies

(a) Satellite formation fly in lunar orbit

To ensure safe operation as well as to maximize observation time, a circular orbit of 300 km altitude (2.3 hour period) is chosen. We find that an inclination angle of about 30° will allow a good three-dimensional distribution of the baseline and a relatively fast precession of the orbit plane, and a good portion of the orbital time would allow the Earth to be shielded. Orbit control and management includes the deployment of daughter satellites, linear array keeping and linear array reconfiguration. The control strategy is based on the objective of balancing and minimizing the fuel consumption of each daughter satellite.

The orbit data of the mother satellite is obtained by ground-based ranging and VLBI, while the relative positions between the satellites are determined by the onboard ISDBA system. With positions relative to the mother satellite measured, the absolute position (i.e. with respect to the Earth-Moon system) of each daughter satellite is also determined.

The control scenarios for the linear array fleet are as follows:

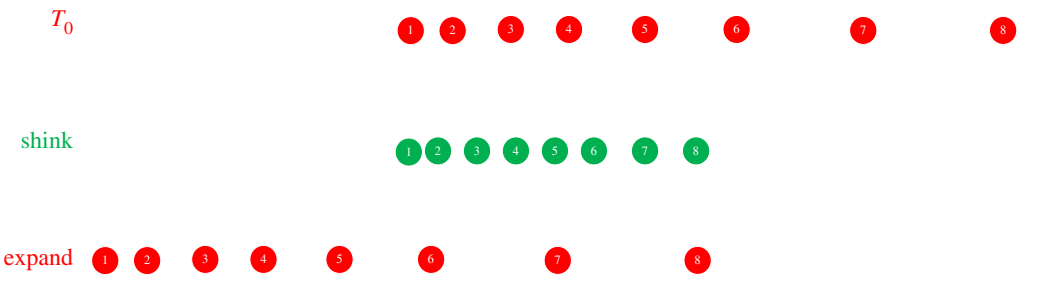

Figure 5. Formation reconfiguration strategy in response to the science requirements. (Online version in colour.)

— Deployment of daughter satellites. When the satellite combination manoeuvred to the 300 km operation orbit, the daughter satellites are ejected one by one from the mother satellites with predetermined time intervals. The release delta-V is about 0.04 m s^{-1}. After about 100 orbital periods (about 10 days), all the daughter satellites are released, forming a linear array configuration.
— Linear array fleet keeping. The main objective of fleet keeping control is to maintain a stable configuration and prevent the collision. Each satellite is kept to fly within its safety box and maintain a stable attitude.
— Linear array fleet reconfiguration. The length of baselines can be varied by reconfiguring the formation. The main consideration in this is to conserve the propellant, and balance the consumption on each satellite. Here a sketch is made of the reconfigurations process:

Step1: keeps S1 stationary, S2–S8 shrinking;
Step2: keeps S8 stationary, S1–S7 expanding figure 5.

To ensure sufficient time for collision avoidance control, it is preferable to move the satellites one after another instead of having them all move simultaneously. The control delta-V can be derived analytically through relative dynamics analysis. The linear array reconfiguration period is about 20 days, and each satellite needs 80 mm s^{-1} delta-V in each linear reconfiguration control period. For the whole mission, there will be about 50 cycles of reconfigurations.

(b) Precision measurement of relative positions and synchronization

We have explored various technologies for relative position determination and data communication. For example, laser technology can provide much larger inter-satellite communication bandwidth and higher precision for ranging and angular position measurement [29], but it is more suitable for point-to-point communication. Communicating with all daughter satellites simultaneously is much harder, and the mass, volume and power consumption requirements are also too high for our daughter satellites. At present, it appears that the microwave technology provides the best solution for our need.

The inter-satellite communication as well as ranging and clock synchronization can all be realized with one microwave link by using the dual one-way ranging (DOWR) principle, and simultaneous operation with all satellites can be achieved easily with frequency division multiplexing. A similar system was developed for the Longjiang satellite experiment [15,30]. Ground tests show that centimetre-sized precision can be achieved in ranging, and the precision of clock synchronization is less than 2 ns. DOWR [31,32] is a simple and effective way to measure the time difference, as shown in figure 6. Time difference multiplied by light speed is equal to the distance between two satellites. The communication frame, bit and phase can be recovered so that the local time difference is measured at the daughter side. Subsequently, the remote time difference measured by the mother is communicated through the inter-satellite link. The real-time difference can then be computed from the remote and local time differences. Random

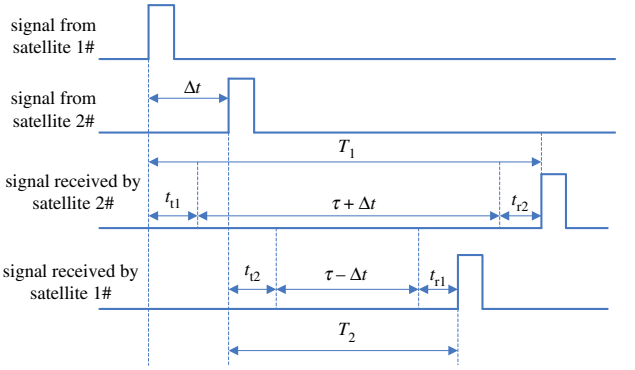

Figure 6. The principle of dual one-way ranging (DOWR) measurement. (Online version in colour.)

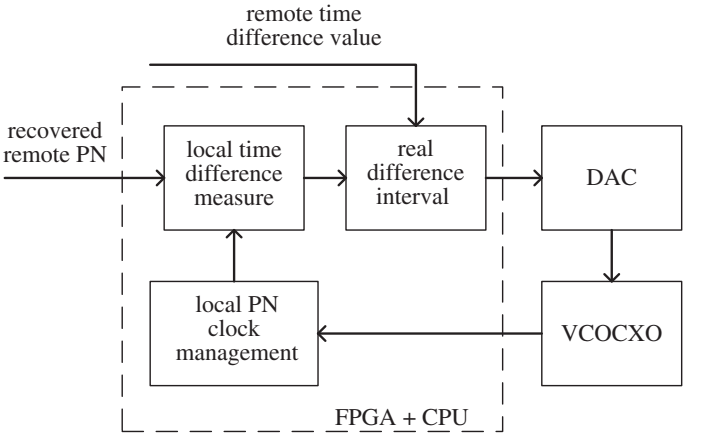

Figure 7. The time discipline process.

jitter in the measurement is reduced by employing a Kalman filter. The distance between the mother and daughter is then obtained by multiplying the real-time differences with the speed of light. After this measurement, the clock on the daughter satellite is synchronized to the clock on the mother satellite by time discipline: a high-precision digital-to-analogue converter (DAC) is employed to adjust the VCOCXO (Voltage Controlled Oven Controlled Crystal Oscillator) by a PID (proportion, integral, derivative) controller, as shown in figure 7. The ranging and clock synchronization are thus realized simultaneously.

The direction of the vector between the daughter and mother satellite is determined by locating the mother satellite position against the star background, and an LED light array (60 W for the 100 km baseline) is carried by the mother satellite as a target, with each daughter satellite using its star sensor camera to take the photograph (figure 8). This method of measurement is not affected by the mechanical installation error of the equipment and satellite attitude error as long as they are within the range to allow normal operation. The angular accuracy is mainly determined by the angular precision of a star sensor camera [33].

(c) High-precision calibration

Calibration of the radio receiver for the DSL mission faces two challenges: first, usually the radio telescope is first calibrated with a strong point source which can dominate the signal received

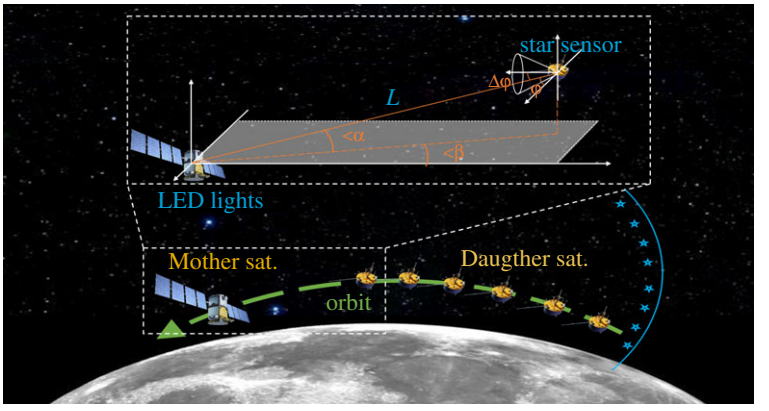

Figure 8. Angular measurement with star sensor camera and LED lights. (Online version in colour.)

by the antenna. But the sky at this band is very bright and do not know what sources there are, so it is unclear whether there are suitable sources to serve as calibrators. Even if there are some very bright point sources, the electrically short antenna has a very broad beam so it is not easy to isolate the effect of the calibrator source from the rest of the sky. Second, the extremely high precision required for the cosmic dawn and dark age measurement is itself very challenging to achieve. To cope with these problems, we consider using an artificial calibration mechanism to ensure the success of the calibration.

To calibrate the instrumental phases of the distributed interferometer array elements, a digitally generated signal can be broadcast from the mother satellite. After this relative phase calibration step, there is still an overall phase undetermined, which must be calibrated with an external source. However, with the relative phase calibration done, even if the astronomical source is dominant, it may still be possible to extract its fringes in the visibility data and determine the remaining phase.

For the cosmic dawn spectrum measurement, the main concern in the design of the antenna is to minimize the chromaticity, i.e. the variation of the beam with frequency. The resonance frequency is outside the observation band for electrically short antenna, making the frequency response smoother. The receiver can be calibrated by switching to several different modes. For example, two-point calibration is performed by injecting hot and warm noise generated from highly stable white noise sources, to determine receiver amplitude response. The impedance mismatch within the system must also be considered: the antenna output and receiver impedances can be measured in-orbit to establish the receiver transfer function. Short/long cables with open, short and load terminators are also used to calibrate the system parameter. System stability is also improved by having a high-precision thermal control subsystem which should provide good control of $\pm 0.1^{\circ}$C. Figure 9 shows a diagram of the receiver channel with a calibration subsystem. However, achieving the required precision is still a great challenge, which requires further study on the possible systematics and their mitigation.

(d) Imaging algorithm with a large field of view, three-dimensional baseline distribution and time-dependent blockage

The imaging for a lunar orbit array is facing a number of complications. The eight daughter satellites will each be equipped with three orthogonal dipole antennas, which are sensitive to the full, 4π steradians of the sky. If a telescope has a small FoV, the sky can be approximated as a plane and images synthesis is simply a Fourier inverse transform of the calibrated visibilities. Many methods have been developed to deal with large FoV [34], but these algorithms were all designed for ground-based arrays, for which there is always a ground-screen (either part of the

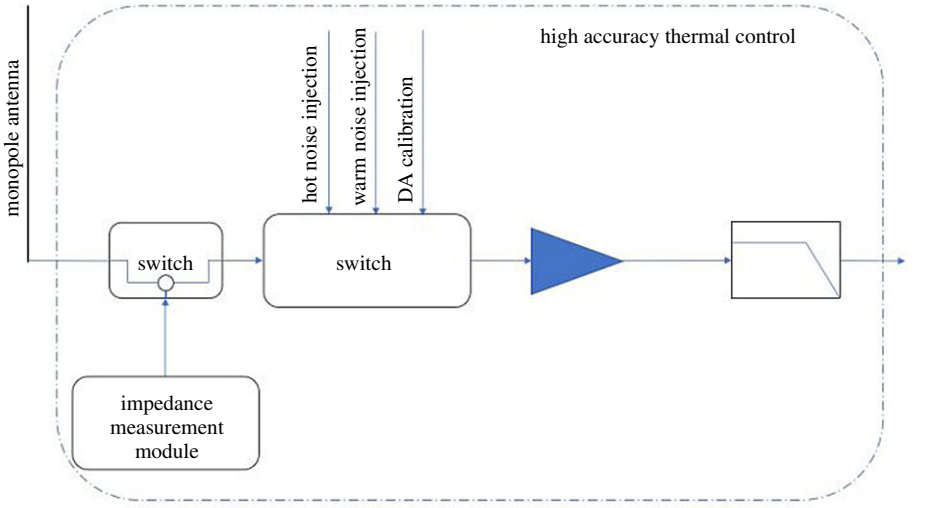

Figure 9. The receiver channel with calibration subsystem. (Online version in colour.)

instrument or the Earth itself) that restricts the FoV to at most half of the sky. Here sources on both sides of the orbital plane are in view, resulting in a 'mirror symmetry' problem. However, as the orbital plane processes in the gravitational field of the Moon and the Earth, a three-dimensional distribution of baselines will be formed. This will complicate the sky reconstruction process as the so-called 'w-term' cannot be neglected, but the mirror symmetry is broken. New imaging algorithms need to be developed [17], which are likely to be computationally expensive as they will need to make use of the full three-dimensional distribution of u,v,w points.

Another complication comes from the continuous motion of the space-based array. With an orbital period of 2.3 h, the u,v,w coordinates are changing much faster than a ground-based array. Hence, for the interferometric observation, the integration time must be very short (38 ms) to avoid time decorrelation. Also, unlike a ground-based array where the relative positions are stable and can be measured with very high precision, the baselines of our array are constantly changing and measured with limited precision, which will also degrade the imaging quality.

(e) Electromagnetic interference suppression and removal

With the RFIs from the Earth shielded by the Moon, the spacecraft itself becomes the main source of RFI. Self-generated RFI is best tackled in the design phase, as reducing these emissions in existing designs is very difficult and costly. The DSL working frequency range is 0.1 MHz–120 MHz (interferometry in 0.1 MHz–30 MHz and spectral in 30 MHz–120 MHz), while the RFIs from the electronics also often fall within this low-frequency band.

Strong RFIs are found at the switch frequencies of the DC-DC module, the frequency of the clock, data bus, etc. Systematic electromagnetic interference (EMI) attenuation techniques are applied to control the EMI from the sources level. In the design of the PCB boards, EMI simulation will be used to keep the signal integrity, EMI filters will be used in the connectors to minimize the radiation from the cable connections, and the satellite platform and payload will have a carefully designed EMI shielding structure. The RFI frequency management, e.g. deriving the various oscillators in different components from the same master oscillator, can reduce the RFI contamination to a limited number of frequencies. In addition, choosing narrow

scientific observational frequency channels (down to kHz level, if the system budget allows this) is advantageous as this would allow excising narrow band RFI.

In terms of algorithmic RFI mitigation approaches, there are many ways to detect and suppress RFI. Intermittent RFI can be detected using a power detector or higher order statistics (kurtosis, cyclo-stationarity), although the latter may require significant computing resources, and may not be available on-board. For multiple antennas on a spacecraft (two or three orthogonal dipoles polarization, or a number on monopole antennas), one can also use spatial filtering to suppress RFI. It may be advantageous to add an additional (small) reference antenna. As it is possible to find a direction of arrival (DoA) with just one set of co-located antennas (using goniopolarimetry), it is also possible to suppress signals from a certain DoA. This principle, to some extent, is also applicable to RFI generated by the spacecraft itself.

5. Conclusion

The ultra-long wavelength radio signals have great potential for a scientific breakthrough, especially for the study of the cosmic dawn and dark ages. Imaging the neutral hydrogen distribution during the dark ages can provide valuable information about the primordial density perturbations and the inflationary origin of the Universe, but this requires extremely large arrays on the far side of the Moon. A useful and practical first step is to map the foreground which is necessary for the design of future dark ages experiments, and to measure the global spectrum with high precision, which gives a first peek of the cosmic dawn and dark age. This first step can be made in the coming decade with a lunar orbit array such as the DSL. The technologies required by such a mission are being developed. International collaboration would enrich and advance these studies. The coming decade offers a unique opportunity for RF-quiet astronomical observations from the lunar far side, before further development of lunar assets compromises the RF-quiet character in the long term.

Data accessibility. This article does not contain any additional data.

Authors' contributions. X.C. is the PI of the project and the primary author of this paper. J.Y. is the technology chief and contributed to the discussion on the key technologies. L.D., F.W., L.W. and L.Z. contributed to the part on key technologies; Y.X. contributed to the part on science and the part on key technologies. All authors read and approved the manuscript.

Competing interests. We declare we have no competing interests.

Funding. The DSL project is supported by the Chinese Academy of Science Strategic Priority Research Program XDA15020200. Additional support for the research at NAOC is provided by Chinese Academy of Science through grant QYZDJ-SSW-SLH017, NSFC through grants 11633004, 11973047, 11761141012 and 11653003.

Acknowledgements. We thank Linjie Chen, Ailan Lan, Maohai Huang, Qizhi Huang, Yuan Shi, Guanqun Song, Shijie Sun, Zhugang Wang, Ji Wu, Bin Yue, Mo Zhang, Fei Zhao and Chengguang Zhu for discussions.

References

1. Cane HV, Whitham PS. 1977 Observations of the southern sky at five frequencies in the range 2–20 MHz. *MNRAS* **179**, 21. (doi:10.1093/mnras/179.1.21)
2. Cane HV. 1978 A 30 MHz map of the whole sky. *Aust. J. Phys.* **31**, 561. (doi:10.1071/PH780561)
3. Reber G. 1994 Hectometer radio astronomy. *J. R. Astron. Soc. Can.* **88**, 297.
4. Brown LW. 1973 The galactic radio spectrum between 130 and 2600 kHz. *ApJ* **180**, 359. (doi:10.1086/151968)
5. Alexander JK, Novaco JC. 1974 Survey of the galactic background radiation at 3.93 and 6.55 MHz. *AJ* **79**, 777. (doi:10.1086/111608)
6. Alexander JK, Kaiser ML, Novaco JC, Grena FR, Weber RR. 1975 Scientific instrumentation of the Radio-Astronomy-Explorer-2 satellite. *A&A* **40**, 365.
7. Novaco JC, Brown LW. 1978 Nonthermal galactic emission below 10 megahertz. *ApJ* **221**, 114. (doi:10.1086/156009)

8. Lazio J *et al.* 2017 The sun radio space imaging experiment (SunRISE). In *XXXIInd General Assembly and Scientific Symposium of the International Union of Radio Science (URSI GASS)*. See https://ieeexplore.ieee.org/document/8105279.
9. Su Y, Li C, Li J, Liu B, Yan W, Zhu X, Zhang T. 2019 In-orbit Performance of Chang'e-4 Low Frequency Radio Spectrometer. In *EPSC-DPS Joint Meeting 2019, held 15–20 September 2019 in Geneva, Switzerland*, id. EPSC-DPS2019-529.
10. Burns JO *et al.* 2017 A space-based observational strategy for characterizing the first stars and galaxies using the redshifted 21-cm global spectrum. *The Astrophysical Journal* **844**, 33. (doi:10.3847/1538-4357/aa77f4)
11. Burns JO *et al.* 2019 Dark Cosmology: Investigating Dark Matter & Exotic Physics in the Dark Ages using the Redshifted 21-cm Global Spectrum. (https://arxiv.org/abs/1902.06147)
12. Kassim NE, Weiler KW (eds). 1990 Low Frequency Astrophysics from Space. In *Proceedings of an International Workshop held in Crystal City, VA, 8–9 January 1990, Springer-Verlag*. (doi:10.1007/3-540-52891-1).
13. Chen X. 2005 Some thoughts on developing our country's space-based low frequency radio astronomy. In *Proceedings of the second academic annual meeting of the deep space exploration branch of the Chinese Aerospace Society*, 49.
14. Cecconi B *et al.* 2018 NOIRE Study Report: Towards a Low Frequency Radio Interferometer in Space. In *2018 IEEE Aerospace Conference, March*, pp. 1–19. IEEE. (doi:10.1109/AERO.2018.8396742).
15. Xibin CA, Jinxiu ZH, Xuelei CH, Junshe AN 2017 Formation flying around lunar for ultra-long wave radio interferometer mission. *J. Deep Space Exploration* **4**, 158–165. (doi:10.15982/j.issn.2095-7777.2017.02.009)
16. Boonstra AJ *et al.* 2016 Discovering the sky at the Longest Wavelengths (DSL). In *2016 IEEE Aerospace Conference*, 1. (doi:10.1109/AERO.2016.7500678)
17. Huang Q, Sun S, Zuo S, Wu F, Xu Y, Yue B, Ansari R, Chen X. 2018 An imaging algorithm for a lunar orbit interferometer array. *AJ* **156**, 43. (doi:10.3847/1538-3881/aac6c6)
18. Chen X *et al.* 2019 Discovering the Sky at the Longest Wavelengths with Small Satellite Constellations. (https://arxiv.org/abs/1907.10853)
19. Cong Y et al. In preparation.
20. Cordes JM, Lazio TJW. 2002 NE2001.I. A New Model for the Galactic Distribution of Free Electrons and its Fluctuations. (https://arxiv.org/abs/astro-ph/0207156)
21. Chen X, Miralda-Escude J. 2004 The spin-kinetic temperature coupling and the heating rate due to lyman alpha scattering before reionization: predictions for 21 cm emission and absorption. *ApJ* **602**, 1. (doi:10.1086/380829)
22. Chen X, Miralda-Escude J. 2008 The 21 cm signature of the first stars. *ApJ* **684**, 18. (doi:10.1086/528941)
23. Bowman JD *et al.* 2018 An absorption profile centered at 78 MHz in the sky-averaged spectrum. *Nature* **555**, 67. (doi:10.1038/nature25792)
24. Barkana R. 2018 Possible interaction between baryons and dark-matter particles revealed by the first stars. *Nature* **555**, 71. (doi:10.1038/nature25791)
25. Bradley RF, Tauscher K, Rapetti D, Burns JO. 2019 A ground plane artifact that induces an absorption profile in averaged spectra from global 21 cm measurements, with possible application to EDGES. *ApJ* **874**, 153. (doi:10.3847/1538-4357/ab0d8b)
26. Tauscher K, Rapetti D, Burns JO. 2020 Formulating and critically examining the assumptions of global 21-cm signal analyses: How to avoid the false troughs that can appear in single spectrum fits. (https://arxiv.org/abs/2005.00034)
27. Bassett N, Rapetti D, Burns JO, Tauscher K, MacDowall R. 2020 Characterizing the Radio Quiet Region Behind the Lunar Farside for Low Radio Frequency Experiments. arxiv:2003.03468.
28. Jester S, Falcke H. 2009 Science with a lunar low-frequency array: From the dark ages of the Universe to nearby exoplanets. *New Astron. Rev.* **53**, 1. (doi:10.1016/j.newar.2009.02.001)
29. Tan LY, Chen YH, Zhao L. 2019 Optimal coupling condition analysis of free-space optical communication receiver based on few-mode fiber. *Opt. Fiber Technol.* **53**, 102004. (doi:10.1016/j.yofte.2019.102004)
30. Zhou L, An J, Wang Z, Wu L, Zhao F, Zhang J, Kong X. 2018 A compact payload system for two formation-flying microsatellites in the CHANG'E IV mission. In *IEEE Aerospace Conference Proceedings*, pp. 1–8: IEEE2018.

31. Kim J. 2007 Measurement time synchronization for a satelliteto-satellite ranging system. In *International Conference on Control, Automation and Systems*, pp. 190–194.
32. Wang Z. 2017 Research on Spaceborne High Precision Ranging and Time Synchronization, Universtity of Chinese academy of sciences, 2017.
33. Xing F, You Z, Dong Y. 2010 A rapid star identification algorithm based-on navigation star domain and K vector. *J. Astronautics* **31**, 2302–2308.
34. Shaw JR, Sigurdson K, Pen U-L, Stebbins A, Sitwell M. 2014 All-sky interferometry with spherical harmonic transit telescopes. *ApJ* **781**, 57. (doi:10.1088/0004-637X/781/2/57)